Polymer 52 (2011) 3717–3724

Contents lists available at ScienceDirect

Polymer

journal homepage: www.elsevier.com/locate/polymer

High-performance poly(2,3-diphenyl-1,4-phenylene vinylene)-based polymer light-emitting diodes by blade coating method

Yung-Ming Liao [a], Hung-Min Shih [a], Kuang-Hui Hsu [a], Chain-Shu Hsu [a,*], Yu-Chiang Chao [b], Sheng-Chia Lin [b], Chun-Yao Chen [b], Hsin-Fei Meng [b]

[a] Department of Applied Chemistry, National Chiao Tung University, Hsinchu 30010, Taiwan, ROC
[b] Institute of Physics, National Chiao Tung University, Hsinchu 30010, Taiwan, ROC

ARTICLE INFO

Article history:
Received 30 March 2011
Received in revised form
15 June 2011
Accepted 18 June 2011
Available online 25 June 2011

Keywords:
Electroluminescence
Gilch polymerization
Polymer light-emitting diodes

ABSTRACT

A new series of super high brightness and luminance efficient poly(2,3-diphenyl-1,4-phenylene vinylene) (DP-PPV)-based electroluminescent (EL) polymers containing methoxy or long branched alkoxy chains were synthesized via Gilch polymerization. The branched alkoxy groups were introduced to enhance solubility for blade and spin-coating processes. Monomers of DMeO-PPV and m-Ph-PPV were used to increase steric hindrance and prevent close packing of the main chain. By controlling the feeding ratio of different monomers during polymerization, DP-PPV derivatives with high molecular weight were obtained. All synthesized polymers possess high glass transition temperatures and thermal stabilities. The maximum photoluminescent emissions of the thin films are located between 544 and 547 nm. Cyclic voltammetry analysis reveals that the band gaps of these light-emitting materials are in the range of 2.75 −2.84 eV. Blade coating was used to fabricate multilayer polymer light-emitting diodes. A multilayer electroluminescent device with the configuration of ITO/PEDOT:PSS/TFB/**P1**/TPBi/LiF/Al exhibited a very high luminescence efficiency (10.96 cd A^{-1}). The maximum brightness of the multilayer EL device ITO/PEDOT:PSS/TFB/**P3**/CsF/Al reached up to 78,050 cd m^{-2} with a low turn-on voltage (4.0 V). For further investigation, polymer **P3** was blended with **DPPFBNA** to achieve white light-emitting device; the multilayer devices generated a maximum brightness of 1085 cd m^{-2} and a luminance efficiency of 0.75 cd A^{-1}, with CIE coordinates (0.28, 0.33) at 11 V.

1. Introduction

Semiconducting polymers have been intensively investigated for their potential applications in light-emitting diodes [1,2], thin film transitors [3], and solar cells [4]. Polymer light-emitting diode (PLED) has the potential to be more competitive than OLED in many future applications due to its low cost solution process [5,6,7]. The most common fabrication process for PLED is spin coating. However, only 5% of material remains on substrate after spinning and the manufacturing throughput of spin coating is low for large areas, dramatically raising the cost of PLED. More importantly, it has been proved that it is difficult to make polymeric multilayer by spin coating because the solvent of the second layer tends to dissolve the previous one. Blade coating is a common method to form large-area polymer films with micrometer thickness, such as photoresists and color filters [8]. Recently we verified the feasibility of blade coating for high-efficiency polymer light-emitting diodes [9]. Unlike spin coating, the area can be easily scaled up and almost all coating materials can remain on the substrate. Furthermore, it is possible to deposit not only single layer but also multilayer without a buffer liquid. The performance of a single layer PLED is as good as that of the spin coated one. The bilayer PLED is even better than the one created by the liquid buffer method. Hence, blade coating was applied to fabricate PLED devices and enhanced electroluminescent (EL) properties were obtained.

Poly(1,4-phenylene vinylene) (PPV) and its derivatives are some of the most attractive classes of conjugated polymers due to their unique structure and highly electroluminescent properties [10]. Long alkyl chains and/or bulky substituents have been incorporated onto the PPV main chain to improve its solubility in order to cast thin films by solution process. Electron donating/withdrawing groups have also been introduced to adjust the optical and electrical properties. For example, poly[2-methoxy-5-(2′-ethylhexoxy)-1,4-phenylenevinylene] (MEH-PPV) is an orange-red emissive polymer and soluble in common organic solvents [11]; thin films of MEH-PPV can be obtained from a spin-coating process. Cyano-substituted

* Corresponding author.
E-mail address: cshsu@mail.nctu.edu.tw (C.-S. Hsu).

0032-3861/$ – see front matter © 2011 Elsevier Ltd. All rights reserved.
doi:10.1016/j.polymer.2011.06.025

poly(2,5-dialkoxy-1,4-phenylene vinylene) (CN-PPV) is a red emissive polymer with high electron affinities [12,13]. Silyl-substituted PPV is a greenish emissive material with a tendency to be easily charged by electrons rather than holes [14,15]. Synthesis of phenyl/alkoxy-substituted PPV copolymers was first reported by Spreitzer, Becker et al. [16,17] The polymerization was performed via Gilch route using different co-monomer feeding ratios. Introducing the DMeO-PPV and m-Ph-PPV moieties into the polymer main chain resulted in high PL quantum efficiency and PLED fabricated alkoxy-substituted phenyl PPVs showed improved EL performance owing to their good film-forming properties. All copolymers showed high EL efficiency above 10 cd A^{-1} and a low driving voltage (~3.5 V). In addition, very high emission brightness (10,000 cd m^{-2}) was easily achieved by applying a reasonable voltage of 6–8.

In 1997, Hsieh et al. used the Diels–Alder reaction, a synthetic route, to obtain a full conjugated polymer, poly(2,3-diphenyl-1,4-phenylenevinylene) (DP-PPV), which exhibits high photoluminescence efficiency in the solid state [18]. This is a versatile method for preparation of a variety of substituted monomers for PPV. Different substituents were introduced at the C-5 position of the phenylene moiety to modify its properties. For example, highly phenylated DP-PPV was synthesized to further improve PL efficiency [19]. Long alkyl chains were incorporated to improve the solubility of the polymer [20]. Liquid crystalline side chains were also incorporated to achieve polarized emissions [21,22]. By following this synthetic route, monomers containing diverse functional groups are easily synthesized and therefore soluble DP-PPV derivatives with high molecular weights are also easily obtained. Recently, we have reported various types of novel DP-PPV-based copolymers [23,24,25]. Devices using DP-PPV derivatives containing long branched alkoxy or fluorenyl substituents with the configuration of ITO/PEDOT/polymer/Ca/Al exhibited a low turn-on voltage (4.0 V), a high external quantum efficiency (3.39 cd A^{-1}), and the highest brightness found in this survey (16,910 cd m^{-2}) [23].

In the present article, we synthesized three new DP-PPV derivatives (**P1**–**P3**) containing the DMeO-PPV and m-Ph-PPV moieties in the polymer main chain with different feeding ratios. The monomers were copolymerized via the Gilch polymerization method. These copolymers show high molecular weights, narrow polydispersity, good thermal stability, and are easily purified. The electrical and spectroscopic properties of these polymers were systematically investigated. Finally, we demonstrate the feasibility of fabrication PLEDs by blade and spin-coating methods. The working principle of multilayer fabrication process by blade coating was reported previously [9]. To the best of our knowledge, so far, there are no reports focusing on improving device performance by using the blade coating method on organic soluble DP-PPV copolymers. The PLED performance is much better than that reported previously in the literature.

2. Experimental

2.1. Instruments

^{1}H and ^{13}C NMR spectra were recorded on a Varian-300 MHz spectrometer. Mass spectra were obtained using a JEOL JMS-HX 110 mass spectrometer. Size exclusion chromatography was measured using a Viscotek GPC system equipped with a Viscotek T50A differential viscometer, Viscotek LR125 laser referactometer, and a Viscotek VE2001 pump. Three 10 μm American Polymer Column were connected in series in order of decreasing pore size (10^5, 10^4, and 10^3 Å), Polystyrene standards were used for calibration, and THF was used as an eluent. Differential scanning calorimetry (DSC) was performed using a TA Instruments Unpacking the Q Series DSC unit operated at a heating and cooling rate of 10 °C min^{-1}, respectively. Samples were first scanned from 30 to 300 °C; after cooling to 30 °C, they were scanned again from 30 to 300 °C. The glass transition temperature (T_g) was determined from the first heating scan. Thermogravimetric analysis (TGA) was carried out using a Perkin Elmer Pyris instrument. The thermal stabilities of the samples were determined under a nitrogen atmosphere by monitoring their weight losses while being heated at a rate of 10 °C min^{-1}. UV–vis spectra were measured using an HP 8453 spectrophotometer. PL spectra were obtained using an ARC

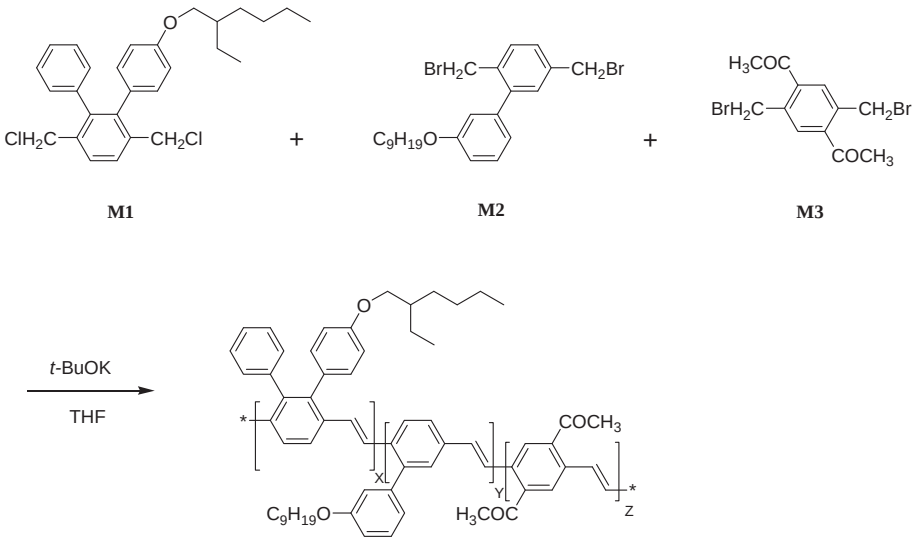

P1, x=90, y=0, z=10

P2, x=85, y=5, z=10

P3, x=70, y=20, z=10

Scheme 1. Synthetic route of the polymers **P1**–**P3**.

SpectraPro-150 luminescence spectrometer. Cyclic voltammetry (CV) measurements were made in acetonitrile with 0.1 M tetrabutylammonium hexafluorophosphate as the supporting electrolyte at a scan rate of 50 mV s^{-1}. Platinum wires were used as both the counter and working electrodes, silver/silver ions (Ag in 0.1 M $AgNO_3$ solution, from Bioanalytical Systems, Inc.) were used as the reference electrode, and ferrocene was used as an internal standard. The corresponding highest-occupied molecular orbital (HOMO) and lowest-unoccupied molecular orbital (LUMO) energy levels were estimated from the onset redox potentials. All the devices were packaged in a glove box and measured in the ambient environment. The current-voltage-luminance characteristics were measured using an optical power meter PR-650 and a digital source meter Keithley 2400. The EL spectra were measured using a Photo Research PR-650 spectrophotometer under ambient conditions after encapsulation.

2.2. Synthesis

Materials: All reagents and chemicals were purchased from commercial sources (Aldrich, Merck, Lancaster or TCI) and used without further purification. Tetrahydrofuran (THF) and dichloromethane were dried by distillation from sodium/benzophenone and calcium hydride, respectively. Monomers **M1**∼**M3** were synthesized as described previously in the literatures [11,16,25,26,27]. The polymer **DPPFBNA** used in white light devices was synthesized according to the literature [28].

2.2.1. Synthesis of polymers *P1*∼*P3*

Different molar ratios of **M1**∼**M3** were used to synthesize polymers **P1**∼**P3** via the modified Gilch method [29]. An experimental procedure for polymer **P3** is given below. To a mixture of **M1** (0.3 g, 0.7 mmol), **M2** (0.1 g, 0.2 mmol), and **M3** (0.03 g, 0.1 mmol) in THF (20 mL), a solution of potassium *tert*-butoxide (1.2 g, 10.6 mmol) in THF (46 mL) was added. The resulting mixture was stirred at room temperature for 14 h under nitrogen atmosphere. The polymer was obtained by pouring the mixture into methanol and filtered. The precipitate was collected by filtration and washed by Soxhlet extraction with acetone, ethyl acetate, and THF, respectively. After filtration and removal of the solvent, the polymer was re-dissolved in THF again and dropped into methanol to form precipitant polymer. The purified polymer was collected by filtration and dried under vacuum for 1 day, resulting as orange-red solid **P3** (0.5 g, 51%). ^{1}H NMR (300 MHz, $CDCl_3$, TMS): $\delta = 0.88-1.90$ (m, 32H), 3.37–4.18 (m, 10H), 6.41–7.60 (m, 20H).

2.3. EL device fabrication

The ITO glasses were degreased in an ultrasonic solvent bath and then dried in a heating chamber at 120 °C. Before transferring the substrate into the glove box, the PEDOT:PSS layer was spin-coated on ITO glass and baked at 200 °C for 15 min in air. It has been reported that thermal annealing of PLEDs can result in improvement of EL performance [30,31,32,33]. Except the emission material in device **F** was annealed in N_2, emission materials in other devices were annealed in vacuum under different conditions. **P1** was annealed at 50 °C overnight, **P2** was annealed at 80 °C for 30 min, and **P3** was annealed at 80 °C for 30 min. For single layer devices (devices **A** and **D**), emission layers were formed on PEDOT:PSS by blade and spin coating with **P1** and **P2** in toluene solution. After the emission materials were bladed from a blade coater with a 60 μm gap, the substrate was then spun immediately to form 50∼60 nm film. As for bilayer devices (devices **B**, **C**, **E**, **F**, **G**, and **H**), TFB (20 nm∼30 nm) was first formed on PEDOT:PSS by blade and spin coating from toluene solution. After TFB was bladed on the PEDOT:PSS, the substrate was then spun at 4000 rpm for 30 s. Immediately TFB was then baked at 180 °C to remove the solvent. The 40∼50 nm thick emission layer about in bilayer devices was then formed by blade and spin coating on TFB. For device **C**, and **H**, a layer of 15 nm TPBI was further formed by blade and spin coating on emission material, and LiF (1 nm)/Al (100 nm) was used as the cathode. Ca (35 nm)/Al (100 nm) was used as the cathode of device **A** and **B**, while CsF (2 nm)/Al (100 nm) was used as the cathode of device **D**, **E**, **F**, and **G**. For white light devices **I** and **J**, a blend of DPPFBNA (400 mg) and **P3** (10 mg) were dissolved in toluene (32 mL) to form 1.5 wt.% polymer solution which was blade-coated onto the PEDOT and TFB layer as emitting layer. CsF (2 nm) Al (100 nm) were used as the cathode for both devices.

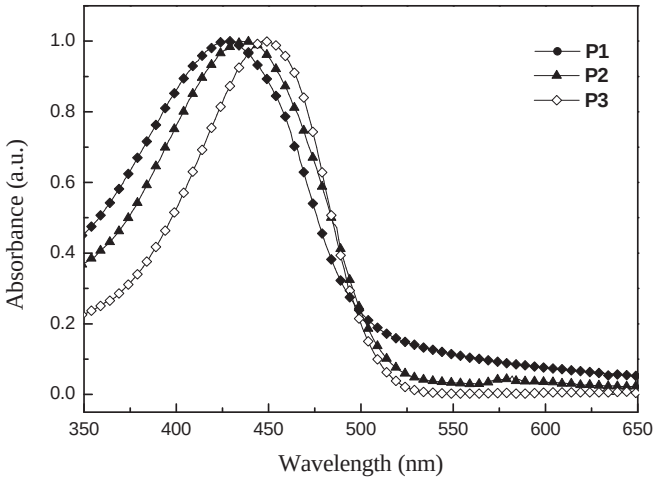

Fig. 1. Normalized absorption spectra of **P1**–**P3** in solid state.

3. Results and discussion

3.1. Synthesis and characterization of the polymers

The synthesis of the copolymers **P1**–**P3** is depicted in Scheme 1. Monomer **M1** has been synthesized in our laboratory according to our previous publications [23,24,25]. We introduced the alkyl substituents into the phenyl ring of DP-PPV so as to minimize gelation and to improve the solubility of the obtained polymers. Monomer **M2** containing a nonoxy substituent linked to the *ortho*-position of 2-phenyl-1,4-bis(bromomethyl)benzene was

Table 1
Feeding ratio and polymerization results of the polymers.

Polymer	x	y	z	Yield (%)	$\overline{Mn} \times 10^5$	$\overline{Mw} \times 10^5$	PDI
P1	90	–	10	56	3.11	4.06	1.31
P2	85	5	10	57	5.62	7.13	1.27
P3	70	20	10	51	2.82	3.57	1.26

Table 2
Thermal, absorption, and emission data of the polymers.

Polymer	T_g (°C)	T_d (°C)	UV–vis (nm)		PL (nm)		ΦPL (%)	
			THF	Film	THF	Film	THF	Film
P1	143	446	442	434	520	544	57	28
P2	135	451	444	440	518	547	55	23
P3	120	414	439	450	516	545	43	28

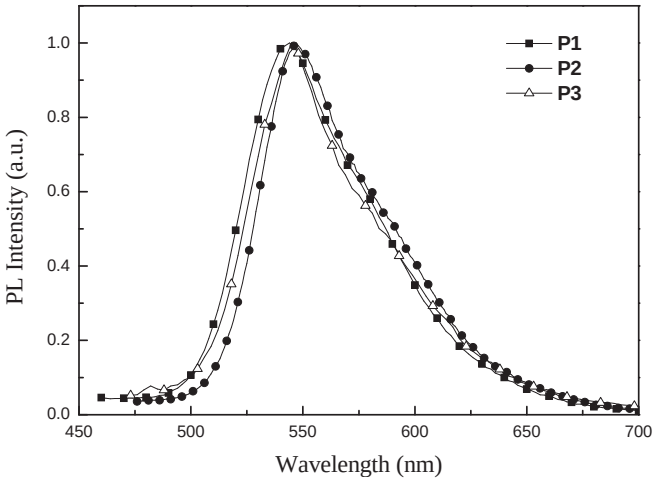

Fig. 2. Normalized PL spectra of **P1**–**P3** in solid state.

synthesized according to the literature methods [26,27]. The MEH-PPV monomer **M3** was prepared as described earlier [11]. It has been reported that incorporation of **M2** and **M3** increases carrier mobility inside the polymer layer [34]. The polymerization was carried out via a modified Gilch route to obtain soluble DP-PPV derivatives. For a typical Gilch synthetic route, α,α-dihalo-*p*-xylene is employed with excess amount of *tert*-BuOK in organic solvents. The monomer feeding molar ratio of **M1**/**M2**/**M3** was 90:0:10, 85:5:10, and 70:20:10, respectively, and corresponding copolymers are denominated as **P1**, **P2**, and **P3**, respectively.

The resultant DP-PPV copolymers are readily dissolved in common organic solvents such as tetrahydrofuran (THF), chloroform, toluene, and chlorobenzene. Their number-average molecular weights (M_n), determined by size exclusion chromatography (SEC, eluent: THF) and calibrated against polystyrene standards, were determined to be 3.11×10^5, 5.62×10^5, and 2.82×10^5 g mol^{-1} for **P1**, **P2**, and **P3**, respectively, with polydispersity index of 1.26–1.31 (Table 1). The thermal properties of the polymers were determined via thermogravimetric analysis (TGA) and differential scanning calorimetry (DSC). All the polymers exhibited good thermal stability with high glass transition temperatures (T_g) over 120 °C and high decomposition

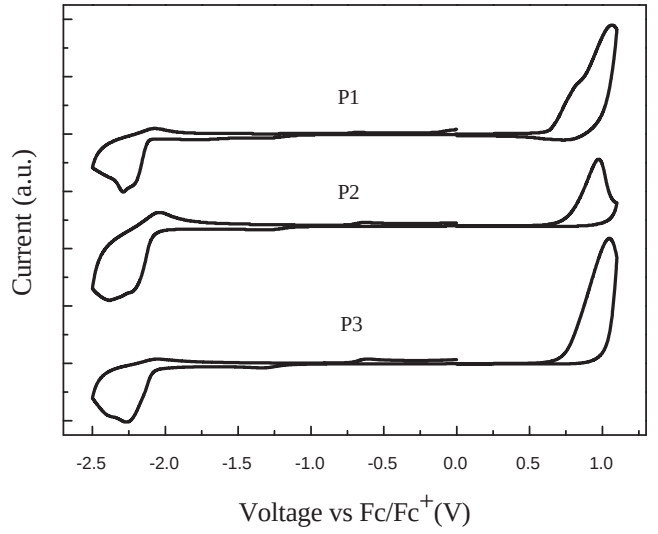

Fig. 3. Cyclic voltammograms of **P1**–**P3** in thin film at a scan rate of 80 mV/s.

Table 3
Electrochemical onset potentials and electronic energy levels of **P1**–**P3**.

Polymer	E_{ox}^{onset} (V)	E_{red}^{onset} (V)	HOMO (eV)	LUMO (eV)	E_g^{ec} (eV)
P1	0.52	−2.22	−5.32	−2.57	2.75
P2	0.65	−2.18	−5.45	−2.62	2.83
P3	0.65	−2.19	−5.45	−2.61	2.84

temperatures (T_d) over 414 °C. Polymers **P1** and **P2** show even higher T_g (>135 °C), which can be attributed to their high molecular weights. Moreover, such a high T_g can prevent morphological changes upon exposure to excessive heat treatment, which is desirable for polymers in the fabrication of light-emitting devices.

3.2. Optical properties

Fig. 1 shows the UV–vis absorption spectra of polymers **P1**–**P3** in thin film. Table 2 summarizes the UV–vis absorption maxima of all polymers in different states. The absorption maxima of synthesized polymers in THF are located in the range of 439–444 nm, which is attributable to the π-π* transition along the conjugated backbone. In comparison with **P1**, the absorption maximum peaks of the thin film absorption spectra of **P2** and **P3** were red-shifted about 6 and 14 nm, respectively, which is consistent with the addition of the feeding ratio of **M2**, where the effective conjugated length is increased because of π-π stacking.

Fig. 2 reveals the PL emission spectra of polymers **P1**–**P3** in thin film. The PL emission maxima in different states are also summarized in Table 2. The maximum emission bands are located from 516 to 520 nm in the solution state and from 544 to 547 nm in the thin film state. A tendency to red-shift from solution to thin film state was also observed. For all synthesized polymers, no significant vibronic band was observed, indicating no or weak chain–chain interactions. The PL quantum efficiencies (Φ_{PL}) of the **P1**, **P2** and **P3** in THF solution are 0.57, 0.58 and 0.43, respectively. By comparing polymers **P1**–**P3**, it was found that Φ_{PL} values were gradually decreased with decreasing feeding ratio of **M1**, implying that the high feeding ratio of **M1** can suppress the formation of aggregates. The results demonstrate that the incorporation of appropriate bulky moieties into polymers brought benefits of high quantum efficiency and decreased chain aggregation.

3.3. Cyclic voltammetry properties

To investigate the information on the charge injection, cyclic voltammogram was used to estimate the HOMO and LUMO energy levels of synthesized polymers. The oxidation and reduction processes are clear and directly associated with the conjugation structure of the polymer. Fig. 3 shows CV of polymers **P1**–**P3** in both processes. The HOMO, LUMO, and energy gap of polymers

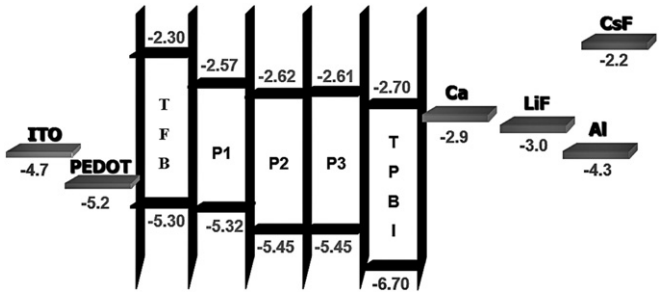

Fig. 4. Energy diagrams of HOMO-LUMO for **P1**–**P3** with device components.

Table 4
Performance of devices A–H.

Device structure (Device No.)	EL λ_{max} (nm)	V_{on} (V)	L_{max} (voltage/V) (cd m^{-2})	efficiency (B/V) (cd A^{-1})
ITO/PEDOT:PSS/P1/Ca/Al (**A**)	552	3.0	6138(9.0)	0.46 (5.5)
ITO/PEDOT:PSS/TFB/P1/Ca/Al (**B**)	548	3.0	8926(9.0)	1.0(5.0)
ITO/PEDOT:PSS/TFB/P1/TPBI/LiF/Al (**C**)	548	5.0	19660(12.5)	10.96(5.5)
ITO/PEDOT:PSS/P2/CsF/Al (**D**)	548	3.0	43160(12.0)	6.58(3.0)
ITO/PEDOT:PSS/TFB/P2/CsF/Al (**E**)	548	3.0	72170(9.5)	6.29(4.0)
ITO/PEDOT:PSS/TFB/P3(N2)/CsF/Al (**F**)	544	4.0	34430(9.5)	3.68(5.0)
ITO/PEDOT:PSS/TFB/P3/CsF/Al (**G**)	548	4.0	78050(10.5)	9.15(4.5)
ITO/PEDOT:PSS/TFB/P3/TPBI/LiF/Al (**H**)	544	4.0	20870(13.5)	7.96(6.0)

P1–**P3** are measured [25] and summarized in Table 3. The energy level diagram of these materials is illustrated in Fig. 4. The HOMO level of the PEDOT layer is known to be ~5.2 eV. Thus, hole injection and transportation from PEDOT to **P1** is expected to be easier than to **P2** and **P3**. It is known that lowering oxidation potential favors hole-injection, which shows advantages for EL applications. As for LUMO levels, **P2** and **P3** have the smaller energy barriers to the Ca or Al cathode than **P1**, implying facilitated electron injection from the cathode to the polymer layer.

3.4. Electroluminescence properties

Eight devices were prepared to study the multilayer device structure, and their device conformation and performance were summarized in Table 4. Different device conformations were made for each polymer in order to find out the best electroluminescence performance. For these multilayer devices, TFB (M_w = 197,000, American Dye Source), which is poly[(9,9-dioctylfluorenyl-2,7-diyl)-co-(4,4′-(*N*-(4-s-butylphenyl))diphenylamine)], was used as the hole-transport layer (HTL) as well as the electron blocking layer (EBL); TPBI, namely 1,3,5-tris(*N*-phenylbenzimi-dazol-2-yl) benzene, possesses both good electron transport characteristic and large IP to block holes. The single layer devices were fabricated by spin-coating method while the multilayer devices were fabricated by blade coating method. Fig. 5 shows the AFM images of **P1**~**P3** films prepared by both spin-coating and blade coating methods. The root-mean-square (RMS) roughnesses of these films were averaged from 6.3 to 1.55 nm; this means that both spin-coating and blade coating method prepared smooth film in the fabrication process.

Initial investigations of the EL properties of **P1** were made by fabricating a single layer device (device **A**) and two bilayer devices (devices **B** and **C**). The EL spectra (a), current density-voltage (b), luminescence-voltage (c), and current efficiency-voltage (d) characteristics of **P1**-based devices are shown in Fig. 6. The positions of the main peak and the vibronic transition peaks under an electric field were very close to those of the corresponding peaks observed in the PL spectra, indicating that the PL and EL properties are very similar. The current density increased exponentially with increasing forward bias voltage, which is a typical diode characteristic (Fig. 6b). The turn-on voltages of the devices **A**, **B**, and **C** were approximately 3.0, 3.0 and 5.0 V, respectively. The maximum brightness of the device **A** was found to be 6138 cd m^{-2} at 9 V, while the corresponding current efficiency was only 0.46 cd A^{-1} at 5.5 V. Device **B** with a structure of TFB/**P1** was fabricated by blade and spin coating on a hot plate for the second layer. The maximum luminance was increased from 6138 to 8926 cd m^{-2} and the device efficiency was enhanced from 0.46 to 1.0 cd A^{-1}. The TFB interlayer plays roles in transporting holes from the PEDOT:PSS layer and blocking electrons at the TFB/emitter interface, resulting in a more balanced electron-hole recombination and the confinement of excitation in the EML [7,35]. The device efficiency was further improved by introducing the electron-transporting interlayer (TPBI) between the EML and the LiF/Al, leading to an efficiency of

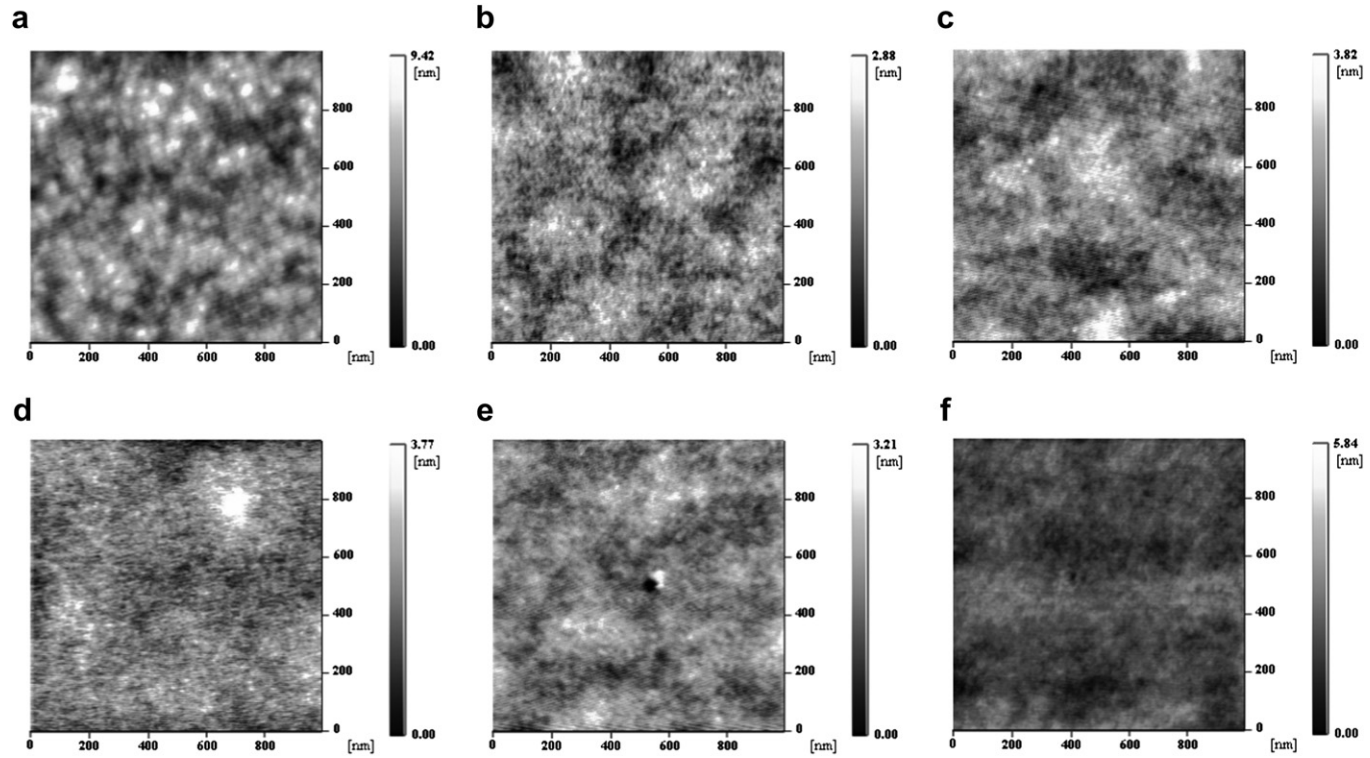

Fig. 5. Topographic AFM images of the films using blade coating for (a) **P1**, (b) **P2**, and (c) **P3** and spin-coating for (d) **P1**, (e) **P2**, and (f) **P3**.

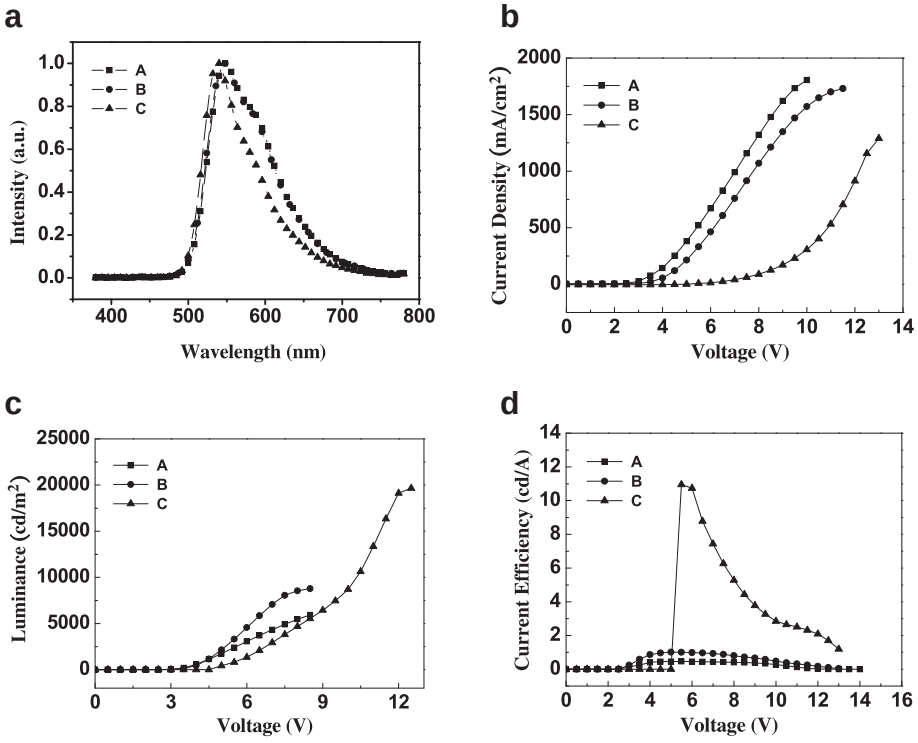

Fig. 6. EL spectra (a), Current density-voltage (*I-V*) (b), luminance-voltage (*L-V*) (c), and current efficiency (*B-V*) (d) characteristics of the **P1**-based devices.

10.96 cd A^{-1} at 5.5 V. The maximum efficiency of device **C** with LiF was 24-fold higher than that of device **A** with Ca. Moreover, the maximum luminance was 19660 cd m^{-2} for the **C** device; it was about 3.2-fold larger than that of the **A** device. The work function of Li (2.5 eV) is lower than Ca (2.9 eV) and, therefore, more efficient electron injection is provided by the LiF/Al cathode. In addition, the presence of the hole/exciton-blocking (TPBI) layer also effectively confines the excitations within the emitting layer, thus preventing

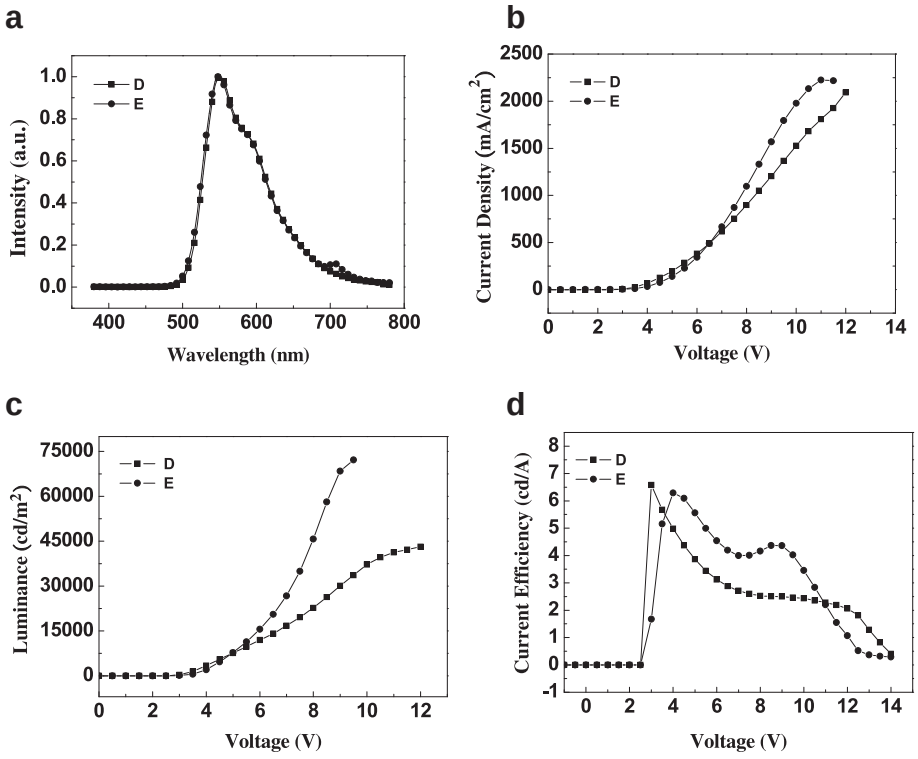

Fig. 7. EL spectra (a), Current density-voltage (*I-V*) (b), luminance-voltage (*L-V*) (c), and current efficiency (*B-V*) (d) characteristics of the **P2**-based devices.

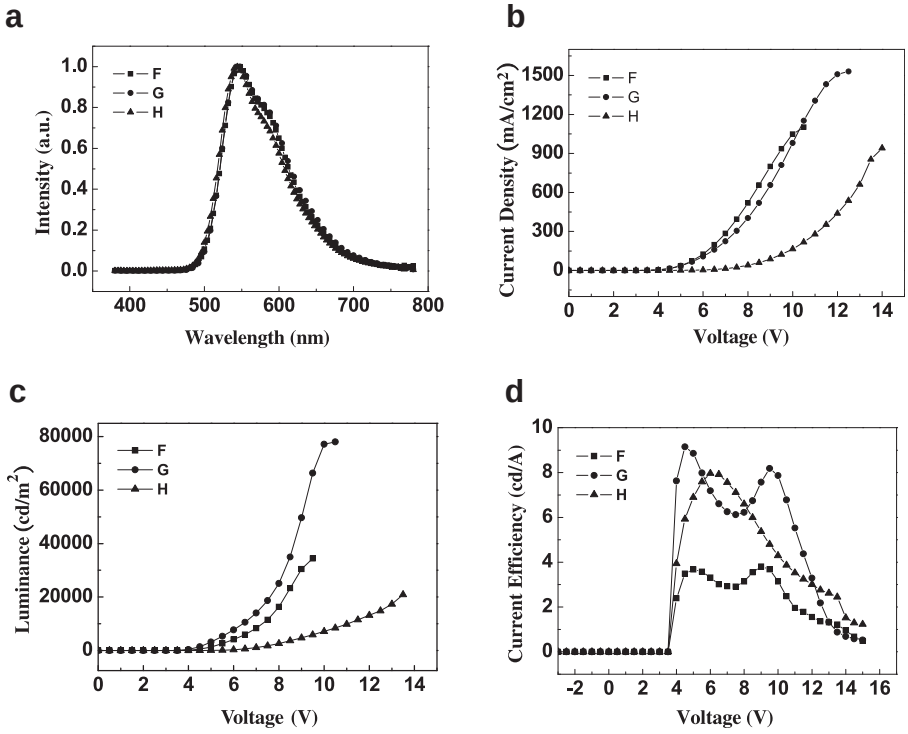

Fig. 8. EL spectra (a), Current density-voltage (*I-V*) (b), luminance-voltage (*L-V*) (c), and current efficiency (*B-V*) (d) characteristics of the **P3**-based devices.

luminescence quenching. Fig. 7 shows the EL spectra and current density-voltage-luminance (*I-V-L*) characteristics of the **P2**-based LED devices. Their EL spectra were also similar to their PL spectra. The current of device **E** was smaller than that of device **D** because the electron current is blocked by the TFB layer. The turn-on voltages for **D** and **E** devices were around 3 V; the maximum luminescence of device **D** was 43160 cd m^{-2} at 12 V, and device **E** with TFB interlayer showed a maximum brightness of 72179 cd m^{-2} at 9.5 V. It can be found that by introducing **M2** into the main chain of **P2**, the **P2**-based devices show a much better device performance than those of **P1**-based devices because of the improved electron-transporting ability of **P2**. Further comparing of the cathodes Ca/Al and CsF/Al in **P1**-based and **P2**-based devices also demonstrated differences. For single layer devices, the maximum efficiency of device **D** with CsF was 14-fold higher than that of device **A** with LiF and reached about 6.58 cd A^{-1}. The efficiencies of the PLED bilayer were 1.0 cd A^{-1} for device **B** with LiF and 6.29 cd A^{-1} for device **E** with CsF; the advantages of using CsF/Al cathode is about 5-fold increase. Owing to the work function of Cs (2.1 eV) being lower than Ca (2.9 eV), more efficient electron injection is provided by the CsF/Al cathode. That is why the efficiency and luminance of devices **D** and **E** were higher than those of devices **A** and **B**. Fig. 8 presents emission spectra and device characteristics based on **P3**, with CsF/Al or LiF/Al as cathodes. The turn-on voltages of **P3**-based devices were about 4 V. Device **G** demonstrated a better EL performance when comparing to device **F** without using N_2 annealing to treat the emissive layer. For device **E** and **G**, the maximum efficiency increased with an increasing feeding ratio of **M2** in the copolymers. Therefore, device **G** achieved certain improvement for the device performance; it showed a great efficiency of 9.15 cd A^{-1} at 4.5 V, and a maximum brightness reaching 78050 cd m^{-2} was observed due to improved electron-transporting ability. This might be the highest value for DP-PPV derivatives reported in the literature so far. As a result, these materials are excellent candidates for PLED and show dramatic potential in further applications.

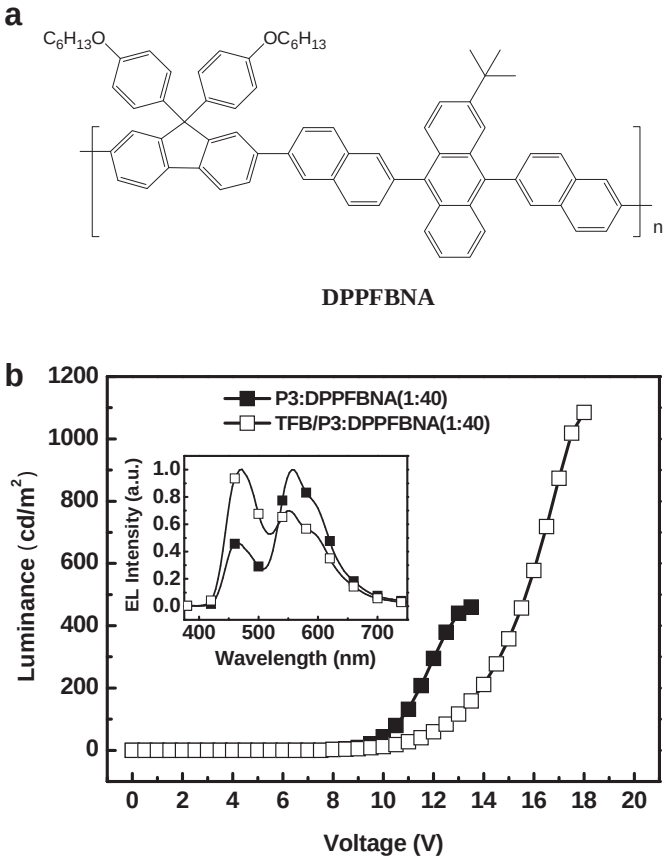

Fig. 9. (a) The chemical structure of **DPPFBNA** and (b) the brightness plots *vs.* voltage for white light-emitting devices. The insert shows the EL spectra at 11 V.

Table 5
Performance of **P3** in double-layer and multilayer white light devices.

Device No.	V_{on}[a]	B_{max}	LE_{max}	EL[b]	CIE 1931[b]
	V	cd m^{-2}	cd A^{-1}	nm	(x, y)
Double layer device **I**	7.5	460	0.67	465, 558, 595	(0.37, 0.43)
Multilayer device **J**	7.5	1085	0.75	470, 550, 595	(0.28, 0.33)

Double layer device **I**: ITO/PEDOT:PSS/P3:DPPFBNA(1:40)/CsF/Al.
Multilayer device **J**: ITO/PEDOT:PSS/TFB/P3:DPPFBNA(1:40)/CsF/Al.
[a] Recorded at 1 cd m^{-2}.
[b] Recorded at 11 V.

3.5. Electroluminescence properties for white light devices

To investigate the superior properties of **P3** further, we fabricated two kinds of white light-emitting devices based on the blend of **P3** and **DPPFBNA**, a blue emitting polymer synthesized in our laboratory [28]. The chemical structure of **DPPFBNA** was depicted in Fig. 9a. The double-layered device structure was made with the configuration of ITO/PEDOT:PSS (50 nm)/EML (70–80 nm)/CsF (2 nm)/Al (100 nm), and the multilayer device structure was fabricated with the configuration of ITO/PEDOT:PSS (50 nm)/TFB (20 nm)/EML (50–60 nm)/CsF (2 nm)/Al (100 nm). The EML composite film was prepared from 1.5 wt.% of **P3** and **DPPFBNA** blending solution (**P3**:**DPPFBNA** = 1:40, w/w) and blade-coated onto the PEDOT or TFB layers. Table 5 summarizes the results of the device performances. The TFB/**P3**:**DPPFBNA** composite film produced a maximum brightness of 1085 cd m^{-2} and a maximum luminance efficiency of 1.18 cd A^{-1}. The brightness and luminance efficiency in these multilayer devices were higher than those in double-layered devices. As illustrated in Fig. 9b, the TFB/**P3**:**DPPFBNA** EL spectrum exhibits dual emissions, with normalized blue and yellow emission intensities covering the entire visible region. The CIE coordinates of the EL emission at 11 V are (0.28, 0.33) which are very close to the desired white light coordinates (0.33, 0.33). When we increased the driving voltages, the white emission CIE coordinates remained stable.

4. Conclusions

This study focused on the design and synthesis of highly efficient electroluminescent DP-PPV derivatives through Gilch polymerization. All synthesized EL polymers with high molecular weights exhibited good solubility in conventional organic solvents and possess high thermal stabilities. The maximum PL emission bands of thin films are located between 544 and 547 nm. Importantly, we have developed a way to simultaneously reduce the cost of PLED and at the same time prevent the dissolution between two polymer layers by blade coating. This is a very simple method to fabricate all-solution-processed multilayer polymer devices. A maximum brightness of 78050 cd m^{-2} was achieved. This is the highest value for DP-PPV derivatives reported in the literature so far. The results reveal that these materials are well suitable for the blade coating method and provide a huge potential in large-area and low-cost light-emitting applications.

In addition, we fabricated double and multilayer white light-emitting devices based on the **P3** and **DPPFBNA** blending film. The multilayer devices showed the maximum brightness of 1085 cd m^{-2} and current efficiency of 0.75 cd A^{-1}, with CIE coordinates of (0.28, 0.33) at 11 V. The white emission remained stable at higher driving voltages.

Acknowledgments

The authors thank the National Science Council (NSC) of the Republic of China for financially supporting this research.

References

[1] Burroughes JH, Bradley DDC, Brown AR, Marks RN, Mackay K, Friend RH, et al. Nature 1990;347:539–41.
[2] Lam JWY, Tang BZ. Acc Chem Res 2005;38:745–54.
[3] Katz HE. J Mater Chem 1997;7:369–76.
[4] Chen SN, Heeger AJ, Kiss Z, MacDiarmid AG, Gau SC, Peebles DL. Appl Phy Lett 1980;36:96–8.
[5] Cho TY, Lin CL, Wu CC. Appl Phys Lett 2006;88:111106-1–111106-3.
[6] Huang J, Li G, Wu E, Xu Q, Yang Y. Adv Mater 2006;18:114–7.
[7] Lee TW, Kim MG, Kim SY, Park SH, Kwon O, Noh T. Appl Phys Lett 2006;89:123505-1–123505-3.
[8] Davard F, Dupuis D. J Non-Newtonian Fluid Mech 2000;93:17–28.
[9] Tseng SR, Meng HF, Lee KC, Horng SF. Appl Phys Lett 2008;93:153308-1–153308-3.
[10] Woodruff M. Synth Met 1996;80:257–61.
[11] Braun D, Heeger AJ. Appl Phys Lett 1991;58:1982–4.
[12] Greenham NC, Moratti SC, Bradley DDC, Friend RH, Holmes AB. Nature 1993;365:628–30.
[13] Chen SA, Chang EC. Macromolecules 1998;31:4899–907.
[14] Wang LH, Chen ZK, Kang ET, Meng H, Huang W. Synth Met 1999;105:85–9.
[15] Chen ZK, Huang W, Wang LH, Kang ET, Chen BJ, Lee CS, et al. Macromolecules 2000;33:9015–25.
[16] Becker H, Spreitzer H, Kreuder W, Kluge E, Schenk H, Parker I, et al. Adv Mater 2000;12:42–8.
[17] Jin SH, Jang MS, Suh HS, Cho HN, Lee JH, Gal YS. Chem Mater 2002;14:643–50.
[18] Wan WC, Antoniadis H, Choong VE, Razafitrimo H, Gao Y, Feld WA, et al. Macromolecules 1997;30:6567–74.
[19] Hsieh BR, Wan WC, Yu Y, Gao Y, Goodwin TE, Gonzalez SA, et al. Macromolecules 1998;31:631–6.
[20] Hsieh BR, Yu Y, Forsythe EW, Schaaf GM, Feld WA. J Am Chem Soc 1998;120:231–2.
[21] Li AK, Yang SS, Jean WY, Hsu CS, Hsieh RB. Chem Mater 2000;12:2741–4.
[22] Yang SH, Chen JT, Li AK, Huang CH, Chen KB, Hsieh BR, et al. Thin Solid Films 2005;477:73–80.
[23] Yang SH, Chen SY, Wu YC, Hsu CS. J Polym Sci A Polym Chem 2007;45:3440–50.
[24] Yang SH, Li HC, Chen CK, Hsu CS. J Polym Sci A Polym Chem 2006;44:6738–49.
[25] Chen KB, Li HC, Chen CK, Yang SH, Hsieh BR, Hsu CS. Macromolecules 2005;38:8617–24.
[26] Antoun S, Karasz FE, Lenz RW. J Polym Sci A Polym Chem 1988;26:1809–17.
[27] Neef CJ, Ferraris JP. Macromolecules 2000;33:2311–4.
[28] Shih HM, Lin CJ, Tseng SR, Lin CH, Hsu CS. Macromole Chem Phys 2011;212:1100–8.
[29] Gilch HG, Wheelwright WL. J Polym Sci A Polym Chem 1966;4:1337–49.
[30] Niu YH, Hou Q, Cao Y. Appl Phys Lett 2002;81:634–6.
[31] Kim J, Lee J, Han CW, Lee NY, Chung IJ. Appl Phys Lett 2003;82:4238–40.
[32] Liu J, Guo TF, Yang YJ. Appl Phys 2002;91:1595–600.
[33] Lee TW, Park OO. Adv Mater 2000;12:801–4.
[34] Yu LS, Chen SA. Synth Met 2002;132:81–6.
[35] Kim JS, Friend RH, Grizzi I, Burroughes JH. Appl Phys Lett 2005;87:023506-1–023506-3.